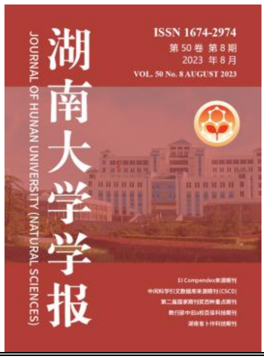

湖南大学学报（自然科学版）
Journal of Hunan University (Natural Sciences)

第 50 卷 第 8 期
2 0 2 3 年 8 月

Available online at http://jonuns.com/index.php/journal/index

Vol. 50 No. 8
August 2023

Open Access Article https://doi.org/10.55463/issn.1674-2974.50.8.14

Safety Gap Factor-Based Lane-Changing Trajectory Planning Model

Md. Mijanoor Rahman[1], Md. Jamal Hossain[2]*, Mohd. Tahir Ismail[3], Majid Khan Majahar Ali[3]

[1] Department of Mathematics, Mawlana Bhashani Science and Technology University, Santosh, Tangail, 1902, Bangladesh

[2] Department of Applied Mathematics, Noakhali Science and Technology University, Noakhali, 3814, Bangladesh

[3] School of Mathematical Sciences, Universiti Sains Malaysia, Penang, 11800, Malaysia

* Corresponding author: z_math_du@yahoo.com

Received: May 8, 2023 / Revised: June 10, 2023 / Accepted: July 16, 2023 / Published: August 31, 2023

Abstract: In discretionary lane changing (DLC) decision models, software-based vehicles should be controlled using safe and comfortable trajectories. The simulated lateral and longitudinal trajectories are approximate trajectories, whereas the calibrated models provide more appropriate trajectories. Very few studies have used the calibration method to find safe and comfortable lateral trajectories at the starting and ending places of lane changing (LC); however, no study has provided safe and comfortable lateral and longitudinal trajectories at these places. This study uses calibrated lateral and longitudinal trajectory models with a comfortable lateral trajectory to pinpoint the safety gap at the target lane during LC. The updated LC trajectory model, in which the adopted lateral and longitudinal trajectory parameters are calculated, is calibrated using a genetic algorithm. This study indicated that the average root mean square error (RMSE) value is 0.93 (*f*) of calibrated data decreasing more than 70%, whereas the average RMSE value of simulation data is 1.93 (*f*). Additionally, the longitudinal positions during LC have an average RMSE value of 0.93 (*f*), while the simulation model's average RMSE value is 1.94 (*f*). Depending on the dataset used, the proposed safety gap can be applied in traffic software while DLC decision models such as binary logistic and game theory models are used.

Keywords: lane changing, transportation planning, gap acceptance, safety factors, game theory model.

基于安全间隙因子的换道轨迹规划模型

摘要：在自主变道（DLC）决策模型中，应使用安全舒适的轨迹来控制基于软件的车辆。模拟的横向和纵向轨迹是近似轨迹，而校准模型提供了更合适的轨迹。很少有研究使用标定方法来寻找变道（液相色谱）起点和终点的安全舒适的横向轨迹；然而，还没有研究提供这些地方安全舒适的横向和纵向轨迹。本研究使用具有舒适横向轨迹的校准横向和纵向轨迹模型来精确定位液相色谱期间目标车道的安全间隙。更新的液相色谱轨迹模型计算了所采用的横向和纵向轨迹参数，并使用遗传算法进行校准。本研究表明，校准数据的平均均方根误差（均方根误差）值为 0.93（f），下降超过 70%，而模拟数据的平均均方根误差值为 1.93（f）。此外，液相色谱期间纵向位置的平均均方根误差值为 0.93 (f)，而仿真模型的平均均

方根误差 值为 1.94 (f)。根据所使用的数据集，所提出的安全间隙可以应用于交通软件，同时使用二元逻辑和博弈论模型等 DLC 决策模型。

关键词：变道、交通规划、间隙接受、安全因素、博弈论模型。

Introduction

In DLC driving situation-based traffic software [1], some decision models such as logistic regression model, game theory model [2], neural networks, support vector machine, and Bayesian filtering [3] use decision factors such as independent and dependent factors [4]. A safety gap trajectory is an independent factor, and DLC decision is a dependent factor.

Planned driver behavior will provide comfort, safety, productivity, and flexibility while lane changing and alleviate numerous transportation issues. Both macroscopic and microscopic factor analyses include these predetermined vehicle movements. The microscopic element distinguishes vehicle trajectory-based motions, such as position, velocity, acceleration, gap, and time headway, whereas the macro factors address traffic flow, density, and average traffic speed [5]. According to the analysis of microscopic factors, the driving mechanism is adaptable and secure. The term "LC driver" refers to a driver of a vehicle who changes lanes. This type of drivers needs to be moving at a high or steady speed and strives to get around any obstacles in the lane. Mandatory LC (MLC) occurs when a driver must change lanes.

To tackle traffic challenges, many academics have created the LC model over the last two decades. Furthermore, discretionary LC (DLC) occurs when a driver modifies his or her lane for a comfortable or safe ride. When driving in places with heavy traffic, the DLC action gives drivers more peace of mind and safety, making them more comfortable when they need to move faster on freeways [6]. DLC participation is not required. Therefore, taking DLC action is safer than taking the LC action that is required. The trajectories of the target rear vehicle (TRV) and the subject vehicle (SV) after LC are used to calculate the safety factor. Researchers have recently created a gap acceptance model with a safety factor and suggested trajectory distribution [7]. An LC vehicle or SV driver typically notices the distance between the front vehicle (FV) and TRV at the target lane following the LC when making a DLC decision. An SV driver uses binary decision when he/she needs a gap in the target lane. TRV drivers may also quickly implement another binary choice (such as a yielding or forbidding decision). When the gap is approved, the SV switches lanes; if not, the SV stays in its current lane. In addition, the TRV either permits or prohibits lane changes.

In LC decision models, the safety gap factor is a key aspect of driver safety [7]. As a result, as a safety indicator, this aspect also has a considerable impact on driver choice. The LC trajectory model can be used to calculate the safety gap factor. However, a few studies have used lateral trajectory models: the quintic Bezier curves [8], a polynomial curve [9], and hyperbolic tangent curve (HTC) [10]. Only small robotic vehicles were used while applying the quintic Bezier curves. The majority of polynomial curves were created using velocity and acceleration. According to [9], velocity and acceleration are considered to be zero at the starting and ending sites of LC. For circumstances with crowded traffic, this assumption, according to [9], is unrealistic. Real views were used to determine HTCs using LC reference angles. Because realistic parameters are employed, the HTC assumption is more plausible than the polynomial curve assumption. The regression coefficient and parameters were used by [10] to successfully fit microscopic-based real data. However, only a small amount of actual data was used to calibrate these parameters and regression coefficients.

Additionally, the majority of the research represented longitudinal movements in safety gap assessment with a straight line. The longitudinal direction does not always follow a straight line when adjusting the vehicle in the target lane, as demonstrated by [9]. After crossing the middle line, the directional straight line includes a weighted parameter that was not calibrated. To establish the safety gap, the longitudinal trajectory line and lateral trajectory HTC parameters were not properly calibrated.

This study determines the safety gap at the target lane during LC by applying calibrated lateral and longitudinal trajectory models with a pleasant lateral trajectory as the minimal curvature at the LC starting and ending positions. The calibration method uses a large dataset (Next Generation Simulation) and a genetic algorithm. The updated LC trajectory model, where the lateral and longitudinal trajectories are chosen, parameters are established using these microscopic data, is likewise calibrated using the genetic algorithm.

1. Literature Review

Vehicle movements on multilane roadways are referred to as LC. When a vehicle driver requires high speed or control and attempts to overcome a barrier in the present lane, he or she switches lanes [14]. This action relates to the LC conduct of the vehicle driver. The LC is classified as required LC or DLC depending on the driver's intentions. For the required LC, the car driver must change lanes. Many academics have created the required LC concept in recent years to solve traffic difficulties (e.g., rear crash, stop-and-go oscillation and working zone signal).

1.1. Lane-Changing Trajectory Model

On both busy and highway roads, DLC activity delivers relaxation and ease [6]. Because of the importance of safety in the DLC model, the safety factor is employed more deeply than in the required LC model. A few researchers have developed the gap acceptance model in recent years, employing safety considerations and trajectory distribution. Prior to LC deployment, the suggested driving behavior is a preplanned activity. The intended action is determined by two factors: lateral and longitudinal directions. Both lateral and longitudinal motions in the coordinate system can arrive at a desired point and detect the gap in the target lane. Therefore, the safety gap in the target lane must be developed and determined using these direction-based LC trajectory models.

In every transportation management, the DLC trajectory planning model is critical for recognizing and assuring safety. The model predicts acceptable gap and dynamic lateral movement trajectories. For more than two decades, the trajectory planning model has been evolving. Several simulation models for DLC trajectory planning have been developed using the quintic Bezier curves [11]–[13], HTC [10], [14], and polynomial curves [9], [15]–[18] for urban and freeway roads. Because the safety factor was calculated using a sine function-based trajectory curve [19], maximum acceleration was applied to construct the unrealistic curve. [9] suggested a trajectory planning curve using PC, where the beginning and finishing locations' reference angles were used to form the trajectory curve. As a result, the polynomial curve is used to form the LC trajectory model. The majority of the LC trajectory models use zero-based velocity and acceleration at the starting and ending positions to derive the PC model, which are false assumptions [9]. The HTC-based model was modified by [10] for trajectory planning. As a result, they proposed using the HTC in required LC and DLC in future studies. Therefore, the purpose of this study is to estimate the safety factor for DLC driver behavior using HTC trajectory planning.

The desired gap point cannot be achieved without the vehicle's longitudinal motions, and the safe distance cannot be determined using the lateral trajectory curve. Only a few studies employ longitudinal movements in the trajectory planning curve to calculate the safety factor. For longitudinal motions, several studies advocated a straight line [19]. However, this straight line may not correspond to actual trajectory vehicle movements during LC. The driver has anticipated places that he or she may desire to reach after LC, and the longitudinal trajectory line direction may change. A previous study has shown that the longitudinal movement line cannot be matched to the longitudinal locations during LC. However, they disregarded the suggestion of organizing longitudinal motions following the requirements. Due to the model accuracy, this longitudinal trajectory planning cannot accurately predict the safety factor during LC. As a result, there is a significant gap in the literature.

1.2. Calibration Method

According to the literature, the simulation model should be enhanced by calibrating it against the actual trajectory data. Otherwise, the model may be useless in the real world. Again, this study fills a research gap in the literature by proposing a trajectory model as a lateral direction curve that is more effective than previous trajectory curves for a pleasant voyage by [10]. The safety gap factor is calculated using trajectory models that are both longitudinal and lateral in nature. Furthermore, the research implies that a longitudinal movement line is required to establish a safety gap in the target lane. However, the literature has significant gaps that may be filled by altering the simulation model of longitudinal motions. As a result of this research, the lateral and longitudinal simulation models appear to perform better when the calibration technique is used. Calibration methods can increase the performance of any simulation model in real-world traffic; the calibration parameters are physically connected to the real-world driving behavior once the model performance is improved [20], [21]. This study has shown from the literature that GA is the most efficient calibration model in traffic research. Furthermore, [10] fitted several parameters to observed data. The calibration procedure may be used to improve the model. [9] suggested a dynamic LC trajectory planning simulation model that utilizes very little data. They agreed that the validation was not sufficiently checked by employing various actual LC trajectories. As a result, further investigation is necessary.

According to [10], trajectory models based on HTC, polynomial curves, and spline-based curves showed similar goodness of fitting values. The model was validated on a few genuine trajectory data. The reason for this is that the linear regression coefficient was utilized in the fitted model, and there were certain data processing restrictions. The authors noted that future studies may enhance their model by incorporating large amounts of traffic data. However, their model only included the lateral trajectory curve during LC. As a result, this study would be changed by adding the longitudinal movement planning model, which must be modified by utilizing large amounts of traffic data. As a calibration method, GA is used to change the aforementioned models. As a result, the purpose of this study is to address a research gap by employing the calibration technique of trajectory planning models.

1.3. Safety Gap Factor

The comfortable LC is represented by the reference angles of the LC beginning and finishing locations, and the gap at the target lane indicates the safety factor during LC. A few studies presented the trajectory curve, which focused on the curvature of its curve as a convenient [10], [19]. Again, some studies offered a gap acceptance model based on LC trajectory planning, in which the safety gap at the target lane was calculated as a safety gap factor [6]. Using a simple calculus formula, the curvature of the trajectory planning curve can be easily computed. However, several researchers formed and recommended other gap acceptance models without using the calibration technique to establish the safety gap factor [22]. This study examines gap acceptance models and calculates the safety gap factor using lateral and longitudinal trajectory planning lines. As a result, the literature on the curvature of trajectory lines and safety gap factor is significant.

2. Materials and Methods

The reference angle is the angle of the driver's vision-based angle of the actual trajectory. By employing this angle during LC, the geometric form of the trajectory curve is shown in [10]. The functional form of the reference angle through LC was planned by [10]. To determine these angles, Equation (1) represents the LC dynamical trajectory values.

$$\theta(t) = \gamma_{lc} \tanh\left(\frac{\sigma}{\frac{l_d}{v_d}}\left(\frac{l_d}{2v_d} - t\right)\right) + \vartheta \qquad (1)$$

where $\gamma_{lc} = \frac{1}{2}\left(\left|\theta_{T_{origin}}\right| + \left|\theta_{T_{target}}\right|\right)$, and $\vartheta = \frac{1}{2}\left(\left|\theta_{(T_{origin})}\right| + \left|\theta_{(T_{target})right}\right|\right)$; t is the time variable; LC starting time is T_{origin}, LC finishing time is T_{target}; reference angles of LC starting and finishing times are $\theta_{T_{origin}}$ and $\theta_{T_{target}}$, respectively, which are represented in Fig. 1. The average positive reference angle of the LC starting and finishing times is γ_{lc}, the average reference angle of LC starting-time and finishing-time is ν. The reference angles, $\nu = 0$ of LC starting-time and finishing-time are equal and opposite. Again, l_d is the total longitudinal displacement during LC, v_d is the average velocity during LC, and σ is an unknown parameter as a lateral aggressive driving behavior.

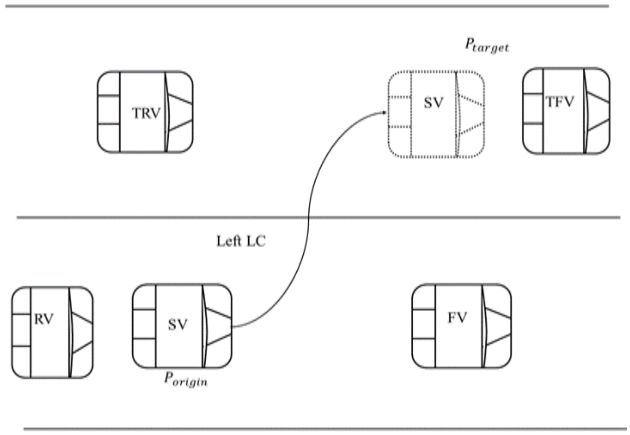

Fig. 1 Starting and ending positions of the SV during LC

2.1. Lateral Position

The initial planning of the lateral trajectory uses the parameters of Equation (1). This equation-based model's computation process is highly simple, efficient, and trustworthy in real-world circumstances. The y-axis is where the lateral displacement occurs. Fig. 1 displays the left LC vehicle's position with the starting and ending times. The lateral position of the real trajectory was fitted by [10] using Equations (2) and (3).

$$\theta(t) = QY(t) + P \qquad (2)$$

Equation (3) is derived using Equations (1) and (2) as follows:

$$Y(t) = \frac{\gamma_{lc}}{Q} \tanh\left(\frac{\sigma}{l_d / v_d}\left(\frac{l_d}{2v_d} - t\right)\right) + \frac{\vartheta - P}{Q} \qquad (3)$$

In addition, Q and P are constants as well as the reference-angle coefficient of the linear regression fitting line of the reference angle and lateral displacement during LC, where the reference angle is the influencing factor, and the lateral displacement is the response variable. These two constants are used by [10], but this research transforms Equation (3) to Equation (4) to relate all parameters with the actual data.

$$Y(t) = S_f \tanh\left(\frac{\sigma}{T}\left(\frac{T}{2} - t\right)\right) + T_f \qquad (4)$$

where S_f is scale factor of HTC that represents the total LC lateral displacement, T is duration of LC and T_f is the abscissa of middle points is represented by the translation factor of HTC. The real trajectory dataset can be used to determine these variables.

2.2. Longitudinal Position

The x-axis represents the direction of the longitudinal displacement. This study's LC decision model combines lateral and longitudinal locations, with Equation (5) being used for the longitudinal position [19].

$$X(t) = x_0 + v_d t,\ for T_{origin} \le t \le T_{target} \qquad (5)$$

[19] mentioned that v_d is average velocity; however, they took LC initial velocity into account to make the model simpler and proposed additional research in the future to make the model better. As a result, this research uses Equations (6) and (7) to enhance the model such that the longitudinal position (simulation position) more closely matches the location of the actual vehicle.

$$X_1(t) = x_0 + \delta_1 u_0 t,\ for T_{origin} \le t \le T_{middle} \tag{6}$$

$$X_2(t) = x_m + \delta_2 u_0 t,\ for T_{middle} \le t \le T_{target} \tag{7}$$

where u_0 is an LC starting velocity, x_0 is an initial longitudinal position, x_m is a middle longitudinal position, T_{middle} is a time, and the driver has passed the middle line separating two lanes. Additionally, the weighted longitudinal direction parameters δ_1 and δ_2 change in order to combine the vehicle into the target lane. When a driver is referred to as a slow driver, the weighted parameter's value is lower than one. Additionally, the weighted parameter has a value greater than one when a driver is described as an aggressive driver. Fig. 2 depicts the aggressive driving style of the driver. Therefore, these weighted factors based on driver aggression are evaluated using actual data.

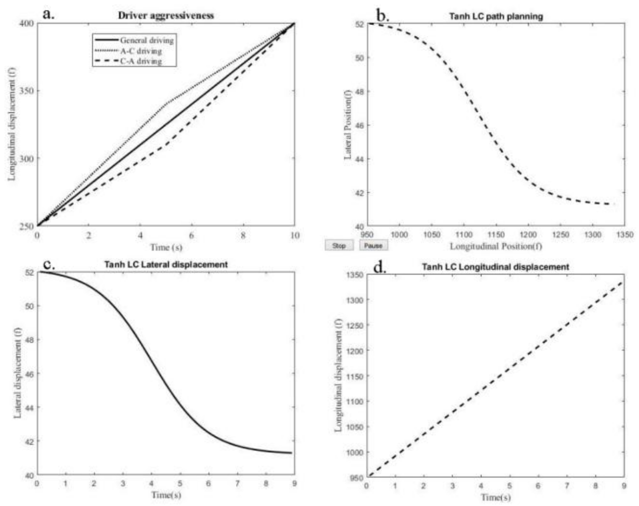

Fig. 2 a. Longitudinal driving aggressiveness; b. Simulation trajectory position of vehicle; c. Lateral position; d. Longitudinal position

In Fig. 2, driving behaviors A-C are first aggressive, then slow, whereas driving behaviors C-A are first slow, then aggressive. In Fig. 2, a straight line represents the general driver's weighted parameter value (one) for longitudinal movements. The dotted line in Fig. 2 depicts similar behaviors when a driver begins driving aggressively and then shifts to a slower speed after passing the middle line. Otherwise, as shown by the dotted line in the same figure, the driver's behavior is first slow and then aggressive. Consequently, by employing these two characteristics, the longitudinal driver movements may better match the actual trajectory in Equations (6) and (7).

2.3. Curvilinear Motion Planning

Curvilinear motion planning provides vehicle coordination along with lateral and longitudinal trajectories during LC. At every time instance, the vehicle stays in a position using these trajectories. This position is assumed by (x(t), y(t)), where the horizontal direction is represented by the x-axis, and the vertical direction is represented by the y-axis. The rectangular coordinate system represents the vehicle longitudinal and lateral positions.

Vehicle coordination with the lateral and longitudinal trajectories during LC is provided by curvilinear motion planning. The vehicle maintains its position using these trajectories at all times. (x(t), y(t)) assumes this position, where the x-axis stands for the horizontal direction and the y-axis for the upward direction. Vehicle longitudinal and lateral positions are represented via the rectangular coordinate system, respectively, x(t) and y(t). Therefore, the position of the vehicle, at any given time t, is $\xi(t)$ = [(x(t), y(t))], where $\xi(t)$ is the cartesian system's position, and t is the time during LC. Equations 3-7 represent horizontal and vertical positions of LC path planning. Fig. 4 and 5 show the relationship between time and lateral and longitudinal positions, respectively. In addition, Fig. 3 shows lateral and longitudinal positions for the simulated vehicle, with the lateral positions placed vertically and the longitudinal ones placed horizontally.

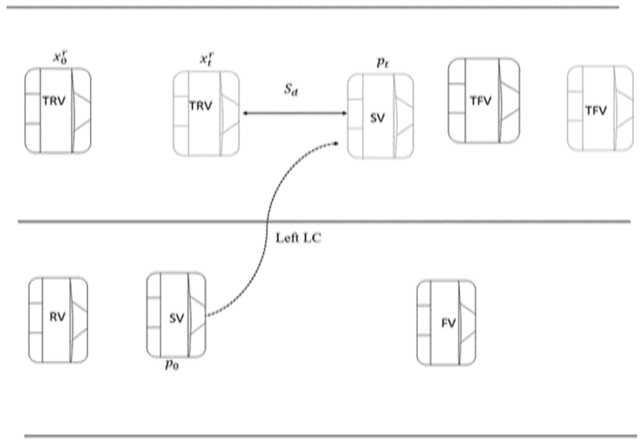

Fig. 3 Rear safety gap

2.4. Curvature

The path's curvature indicates how comfortable the travel will be; a path with a low curvature will be more comfortable [10]. [10] demonstrated that the tanh model's curvature is less than that of other quintic Bezier curves and PCs. However, the vehicle system can determine the curvature at any location by employing the updated parametric curve. The curvature value is determined using Equation (8). The comfortability of the model using the modified lateral and longitudinal position-based parametric lines is justified by this study employing this equation.

$$Curvature, k = \frac{y''}{(1+y'^2)^{2/3}} \quad (8)$$

where y is the lateral position determined from Equation 4; y'' and y' are 2nd order and 1st order derivatives, respectively. These derivatives are with respect to longitudinal vehicle position (see Equations 6 and 7).

2.5. Calibration and Validation Approaches

Equation (4) represents the lateral trajectory, and Equations (6) and (7) represent the longitudinal trajectory for the LC decision model to produce the simulation data. Simulation models are ineffective for planning actual trajectories. These parametric-based trajectory models use the calibration approach to enhance the simulation model. The GA is considered in the study as a calibrating method. The sum of square error (SSE) used in the objective function is displayed in Equation (9). With the exception of the driver's lateral aggressive conduct, all parameter ranges from the dataset are considered in GA because this type of values is not in the dataset. To better fit the real dataset, this research investigates the various values of lateral aggressive behavior.

Additionally, the validation strategy is used to evaluate the effectiveness of the model using Equation (10). The validation function can employ any goodness-of-fit function because of similarity as the calibration approaches use the SSE function. Therefore, the RMSE function is used as the unit of input and output variables in this study. In addition, RMSE determines the simulation model's error when real data cannot be put into the model. In this instance, measuring error can be done using the same unit of input and output variables.

$$\min_{\mu \in \Omega} \sum_{t=1}^{N} [p_n(t \mid \mu) - \hat{p}_n(t)]^2 \quad (9)$$

where Ω is optimum set of parameters, $\mu, p_n(t \mid \mu)$ and $\hat{p}_n(t)$ are simulation and observed positions, respectively, at iteration time *t*.

$$RMSE = \sqrt{\frac{\sum_{t=1}^{N} [p_n(t) - \hat{p}_n(t)]^2}{N}} \quad (10)$$

where t = 1 is LC starting time, and t = N is the LC ending time in Equation (10).

2.6. Safety Gap

Using the longitudinal positions of the FV and SV, this safety gap was computed. For LC trajectory planning, [9] presented the range of safety gaps using RV and FV. In addition, they used the longitudinal location of these cars to compute the safety gap. The presumed rear safety gap is the range of the safety gap with the back vehicle. This research gathers the rear safety gaps of all LC and NLC vehicles to achieve its goal. The longitudinal position of the TRV is calculated by Equation (5) [19]. Here, the longitudinal trajectory model is used to calculate the SV location. When the distance between the SV and TRV is closer than their respective safety gaps, a rear collision between the SV and TRV is possible. The SV may avoid colliding with the TRV if it advances to the target lane while leaving a rear safety gap. The TRV departs from its present lane and adheres to the one-dimensional motion equation during the SV LC (Equation (11)).

$$x_t^r = x_0^r + v_0^r t_{lc} \quad (11)$$

where x_t^r is a rear vehicle position after LC at target-lane, x_0^r is TRV initial position at LC starting time, v_0^r is TRV initial velocity at LC starting time, and t_{lc} is total LC time.

Equation (12) is used to compute S_d, the rear safety gap. Although the lateral position of the SV after LC is not used in safety gap assessment, it is possible to determine the LC finishing time from the lateral position since the SV completes the LC after it has reached the target-lane (the desired lateral position). Due to the same lane, TRV becomes the new rear vehicle of SV when SV enters the target lane. Equation (12) can be used to determine a regarded gap between these two cars in that case.

$$S_d = x(lc) - x_t^r - L_{lc} \quad (12)$$

where L_{lc} is the length of SV, $x(lc)$ is the position of the SV along its longitudinal axis following the LC, and all vehicle lengths are treated equally. It's not usually possible for the SV driver to switch to the LC. This driver is capable of calculating the rear safety gap at the LC's starting position by using Equations (11) and (12).

3. Data Processing

US 101 (Hollywood Freeway), Los Angeles, California, features a road with multiple lanes on either side (Fig. 4). The auxiliary road connects the off-ramp and on-ramp traffic systems on one side. The vehicle trajectories were recorded using cameras set up at the tops of the tall structures. The vehicle trajectories from all lanes of the more than 600-meter road were microscopically captured by these cameras [23]. This dataset, according to [24], is the most widely used and available in traffic research because it contains a vast amount of microscopic data.

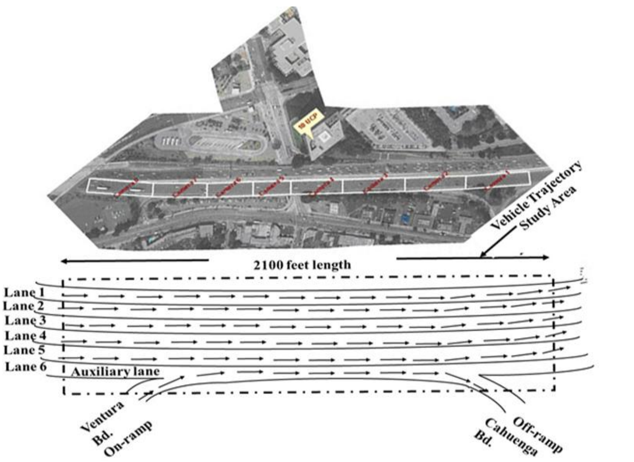

Fig. 4 Data collection area, NGSIM, US-101 [23]

Microscopic factors, including local longitudinal and lateral positions of the SV, global time, vehicle velocity, vehicle acceleration, vehicle lane position, FV, and rear vehicle, were collected. The time-intervals are 7.50-8.05 am, 8.05-8.20 am, and 8.20-8.35 am on June 15, 2005. The total captured number of vehicles at these 45 minutes was 6101 [25]. Compared to other times of the day, the morning has more traffic congestion. The vehicle trajectory contains 10 data points for each microscopic factor per second, with a 0.1-second resolution [25]. The dataset used for this study, which covers the hours of 7.50 am to 8.05 am, contains multiple 1,180,000 row vectors and 18 column vectors in a CSV file. The row information dataset contains 2169 automobiles, and only the DLC vehicles in lanes five through four are identified. Therefore, during the 2100 feet of monitored roadway, there were 123 total DLC vehicles and 9 total NLC incidents. By removing certain incomplete and dubious LC vehicles from the dataset, [26] identified DLC vehicles for lanes one through three.

In this dataset, there are 123 DLC events from Lane 5 to Lane 4. As a result, SV and RV in the present lane and FV and RV in the target lane generate the LC groupings. 123 DLC vehicles and 9 NLC vehicles make up this data set's DLC segment. An NLC vehicle is one that cannot shift lanes to avoid obstacles. This dataset is used to directly monitor NLC vehicles. The NLC vehicle's front side also approaches the center line and reverses to the center of Lane 5. Given that each lane is 11.84 feet wide, the middle line of lanes five and four is 47.36 feet away from the observation point [27].

DLC and NLC cars cannot be distinguished from one another before beginning an activity from the dataset because DLC is optional and depends on the driver's preferences. While an NLC car is unable to alter the current lane, a DLC vehicle can be recognized when it crosses it. Therefore, this study employs the direct method (graphical method) of trajectory plotting by employing MATLAB coding to identify the LC and NLC vehicles (Fig. 5). The direct method was employed in some traffic studies [27, 28].

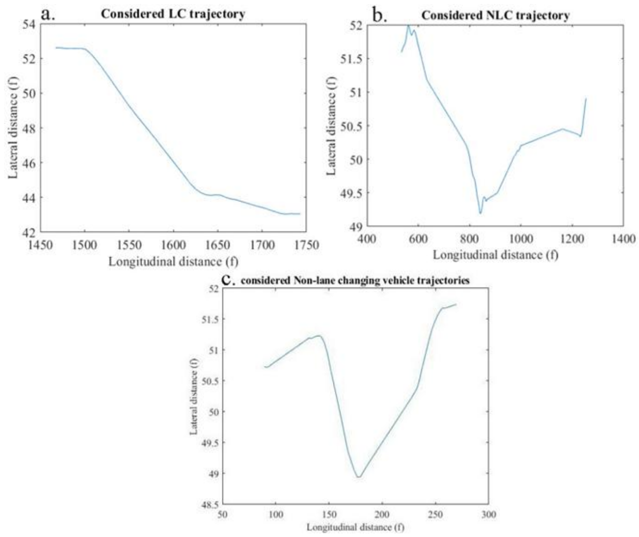

Fig. 5 a. Lane-changing vehicle trajectories; b. Considered as lane changing; c. Considered as non-lane changing

This study focuses on DLC decisions, where LC depends on driver intention but may not always be able to tell them apart from car-following intention. It must be clear that the driver of the car keeps switching lanes when the LC is initiated. Fig. 5(a) shows the SV movements before, after, and during LC, where the LC start is clearly identified. In Fig. 5(b), the vehicle movements during LC are separated from Fig. 5(a). Additionally, Fig. 5(c) displays the NLC situation's trajectory. As a result, this study gathers information about DLC vehicles from 132 instances after the LC activity has begun (123 LC and 9 NLC).

The SV and FV are in the current lane, and the TRV and TFV are in the target lane. Each group contains four vehicles. Each vehicle in a group has acceleration, longitudinal and lateral velocities. The LC starting, finishing, and middle positions of the SV are also included in this dataset. The trajectory data can be used to determine the LC duration. Using the LC time, the average longitudinal velocity and lateral velocity are determined.

4. Result Explanation

The calibration result shows how the modified LC trajectory model was improved when GA was applied to NGSIM data. The parameters of the trajectory model were calibrated to match the actual trajectory. The model vehicle positions, therefore, match real vehicle positions more closely when calibrated parameters are used.

4.1. Lateral Position

Equation (4) involves the parameters T, S_f, σ, and T_f. Driver aggressiveness is σ, total LC time is T_f, middle lateral position of LC is T, and half of the overall lateral length is S_f. The NGSIM dataset contains intervals for the values of these parameters. The midpoint of the lateral positions, maximum lateral positions, and total LC time, which are (46.5 ± 0.5) (f), (52 ± 1) (f), and (10 ± 5) (s), respectively, in the

NGSIM data.

Because it may not be possible to determine the driver's lateral aggressive behavior using the NGSIM dataset, this research analyzes the various ranges of this parameter (Table 1) using the RMSE function. The highly aggressive driving style is represented by the low value of the aggressive parameter because a slow driver might find this behavior uncomfortable [10]. As a result, this study views the aggressive parameter's [2, 8] range as having a lower RMSE value and a larger parameter value.

Every trajectory curve has a different middle coordinate because each trajectory has a different LC position. Aggressive driving, lazy driving, and normal driving behaviors affect the total LC time. Using the calibrated parameters, the average RMSE of the lateral displacement is found to be 0.93 (f) (Table 2).

Table 1 Test of the lateral aggressive parameter range (Developed by the authors)

Parameter	Initial range	Changed (No. of the vehicles)	Calibrated range	RMSE (f)
σ	[0, 10]	3	[.4, 10]	0.93
	[2, 8]	6	[2, 8]	0.93
	[2.5, 7]	13	[2.5, 7]	0.96
	[3, 6]	17	[3, 6]	0.99
	[3, 7]	25	[3, 7]	0.99
	[4, 6]	33	[4, 6]	1.08
	5	All	Simulated	1.93

Table 2 Interval of the parameters (Developed by the authors)

S. No.	Parameter	Initial value	Unit
1	S_f	[5, 6.5]	Feet
2	σ	[2,8]	None
3	T	[5, 15]	Second
4	T_f	[46, 47]	Feet

When employing these intervals and excluding five vehicle datasets from the calibration technique, the average RMSE is 0.76 (f). These five vehicles have quite varied trajectories, with two having high-scale factors and highly aggressive driving styles and three having high-scale factors and very slow driving styles. According to the initial characteristics employed, very lazy driving and a high scale factor are defined. When the aggressive parameter exceeds eight, the driver is driving very slowly, and when the scale factor exceeds fifty-three, the scale factor in this study is large.

The vehicle's lateral displacements along the prediction curve and real trajectory scenario of the NGSIM dataset are shown in Fig. 6(a). The solid and dotted lines, respectively, show the predicted curve and actual trajectory of a vehicle (randomly selected from 123 vehicles). This demonstrates that the parametric curve's lateral displacements are almost identical to those of the actual trajectory curve. Fig. 6(b) only displays one trajectory-fitted curve. The RMSE value is calculated by comparing the measured trajectories with the calibrated curves.

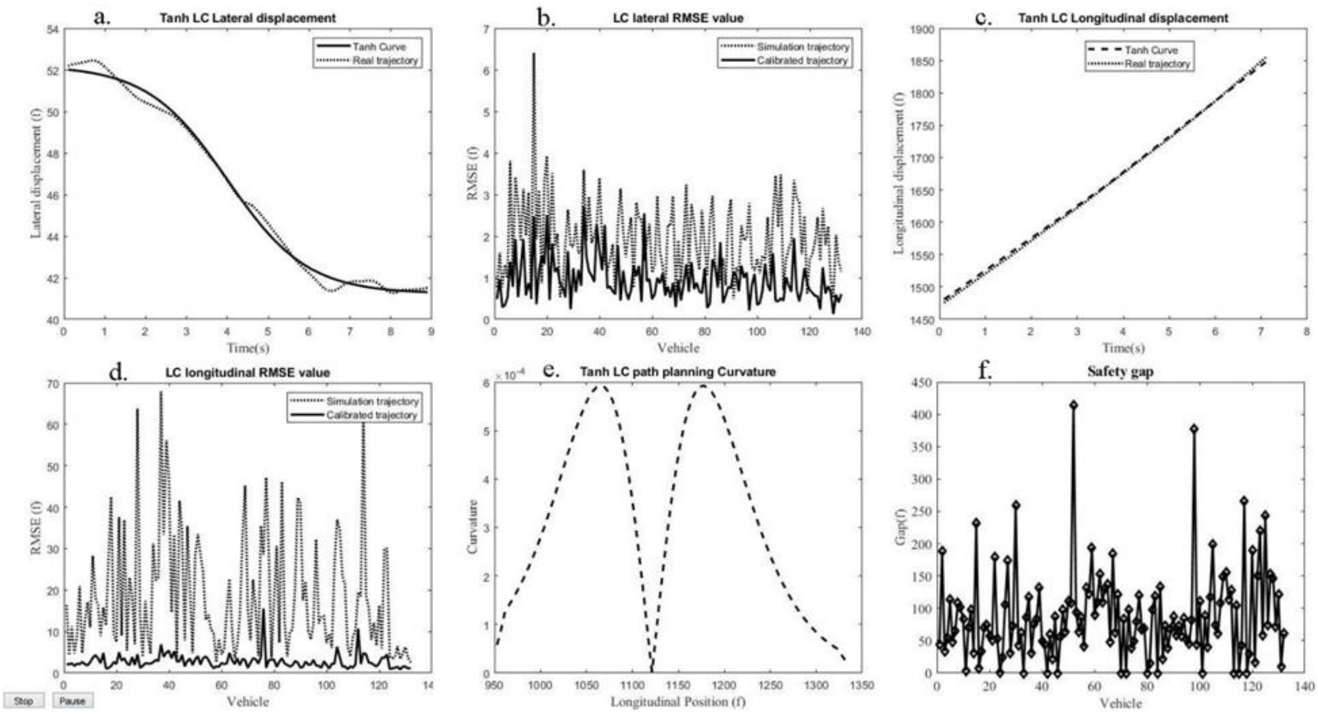

Fig. 6 a. Lateral position; b. Root mean square error value of the lateral movements; c. Longitudinal position; d. Root mean square error value of the longitudinal movements; e. Curvature value; f. Frequency of the safety gap (Developed by the authors)

In Fig. 6(b), the model parameters are calibrated by applying the calibration procedure GA. The RMSE values of the lateral positions are displayed using Equation (10). The lateral position curves were fitted to the trajectory planning of 123 LC and 9 NLC vehicles after calibrating the parameters. The average RMSE value of the calibrated data using all the vehicle trajectory data is 0.93 (*f*) but the average RMSE value of the simulated data is 1.93 (*f*). Thus, Table 2 displays these RMSE values. The simulation model uses the parameter's average value.

4.2. Longitudinal Position

To match longitudinal trajectories against NGSIM datasets, parametric equations (6) and (7) of the longitudinal trajectories are employed. These equations' parameters correspond to aggressive driving behavior. The NGSIM datasets, which contain LC observed trajectories with 123 LC and 9 NLC vehicles, were used to calibrate the longitudinal movements. The longitudinal position lines are adjusted against the actual longitudinal positions of the DLC vehicles. The fitting method calibrates the characteristics of aggressive driving behavior using the GA. This study uses the interval of aggressive driving behavior, as stated in Table 3.

Table 3 The interval of aggressive driving behavior

Parameter	Initial range	Changed (No. of the vehicles)	Calibrated range	RMSE (*f*)
δ_1, δ_2	[0, 2]	1	[0.55, 2]	2.70
	[.2, 1.8]	1	[0.55, 1.8]	2.71
	[.4, 1.6]	4	[0.55, 1.6]	2.72
	[.5, 1.5]	6	[.5, 1.5]	2.75
	[.6, 1.4]	11	[.6, 1.4]	2.86
	[.8, 1.2]	40	[.8, 1.2]	4.13
	1	All	Simulated	19.24

A comparison of the RMSE values for various weighted parameter ranges is shown in Table 4. When intervals [0, 2] and [.2, 1.8] were used, the RMSE value marginally decreased because only one vehicle trajectory contained the interval limiting values [.8, 1.2] and [.6, 1.4]. They suggest that if we consider a wider range, the parameter might rise. The 40 and 11 vehicle trajectories, using parameter intervals [.8, 1.2] and [.6, 1.4], contain the limiting values of the intervals, respectively. Additionally, when intervals [.8, 1.2] and [.6, 1.4] are employed, the RMSE values are much higher than those of the interval [.5, 1.5]. As a result, the initial parameters of the calibration approach as weighted parameter values are in the interval [.5, 1.5].

By comparing actual trajectories, Table 3 also displays the average RMSE (18.38 (*f*)) of the simulated longitudinal displacement. The simulated parameter values are used in this RMSE formula. Furthermore, the calibrated longitudinal position's average RMSE value is 2.76 (*f*) with initial parameters in the interval [.5, 1.5]. As a result, the improved model, which used a calibration approach to improve these parameters, fits real longitudinal movements better.

Fig. 6(d) illustrates the model's efficacy by comparing the RMSE values of the real and modified parametric trajectory data. These outcomes further demonstrate that the improved model produces the vehicle trajectory with accuracy. The calibrated parameters enhance the model's ability to fit against actual data, which includes 123 DLC and 9 NLC vehicles. Because each driver generally exhibits a varied level of driving aggression along longitudinal travel, the parameters of the longitudinal trajectory model must be fitted using actual data. Furthermore, this behavior parameters differ for each trajectory. These tables also include the RMSE values, which were computed using the calibrated and simulated parameters. The RMSE values of the calibrated and simulated lines correspond to the solid and dotted lines, respectively, in Fig. 6(d).

4.3. Curvature

Using Equations (8), (4), and (5), the curvature's maximum value for the longitudinal LC distance (approximately 400 feet) is 0.0006 (Fig. 6(e)). It may exceed this amount if the longitudinal LC distance is less than 400 feet. At the beginning and end of the curve, these curvature values are very close to zero (Fig. 6(e)). [19] concurred that traveling over curves that are close to zero at either the starting or finishing points is pleasant. This updated trajectory curve's maximum curvature value (Equation (4)) is less than maximum curvature value found by [10]. This lateral curve was modified in this study using the calibration approach (GA). This improved trajectory curve shows that the lateral position is more accurate. To further determine the continuous curvature, a modified lateral curve and a simulated longitudinal line were used.

The calibrated longitudinal line may be used in future studies to measure continuous curvature. [10] discovered curvature values (2×10^{-4}) at the LC starting and ending points; however, a modified trajectory curve showed curvature values (less than 6×10^{-5}) at the same locations. Therefore, at employing the improved lateral trajectory curve, the curvature at the starting and finishing sites decreases by more than 70%. Therefore, this model may be used to calculate the safety gap and is effective for a comfortable ride. The spots during LC are discovered at 0.93 (*f*), while the simulation model's average RMSE value is 1.94 (*f*).

4.4. Safety Gap

Equations (11) and (12) were used by [9] to modify the range of the safety gap using TRV and TFV for LC trajectory planning. The same equation used to calculate the rear safety gap is also used to calculate the safety gap between SVs and TRVs following LC. For this goal, 123 LC and 9 NLC rear safety gaps were collected in this study. The possibility of a rear collision between SVs and TRVs exists when the distance between them is less than the safety gap. The TRV may not collide with the SV if the SV shifts to the target lane with the rear safety gap. Fig. 6(f) displays the safety gaps.

The safety gap at the target lane during LC is depicted in Fig. 6(f). In the same figure, the vertical number denotes the distance between the SV and TRV following LC. Negative values are treated as zero because they represent a model error and an unreasonable value for the gap. The majority of SV drivers during LC are aware of the bigger safety gap; hence, this aim sums up that the safety gap is more significant for SVs to change lanes [22], [27].

5. Conclusion

In DLC driving situation-based traffic software, decision models such as logistic regression, game theory, machine learning, or deep learning-based stochastic models use decision factors such as independent and dependent factors. The safety gap trajectory is an independent factor, and the DLC decision is a dependent factor. When considering the longitudinal distance, the curvature values at the lane-changing (LC) starting and terminating points (approximately 400 (*f*)) are less than 6×10^{-5}. It might grow if the true longitudinal distance is less than 400 (*f*). These curvature values are lower than those discovered by [10]. The calibration results indicate that while the average RMSE value of the simulation model is 1.94 (*f*) the average RMSE value of the lateral positions during LC is found to be 0.76 (*f*) and the average RMSE value of the longitudinal positions during LC is found to be 0.93 (*f*). Furthermore, when comparing actual trajectories, the average RMSE value of the simulated longitudinal displacement is 18.38 (*f*). The average RMSE of longitudinal displacement is 2.76 (*f*) after calibration. Decision models can be theoretically developed by using the safety gap factor. Whereas this study only develops decision models without theoretical development and depends on used dataset. Further, this study gathers the safety gap for subject vehicles at the target-lane using the proposed trajectory models. The proposed models can be used in future studies to DLC decision.

References

[1] MORIDPOUR S., SARVI M., ROSE G., and MAZLOUMI E. Lane-changing decision model for heavy vehicle drivers. *Journal of Intelligent Transportation Systems: Technology, Planning, and Operations*, 2012, 16(1): 24–35. https://doi.org/10.1080/15472450.2012.639640

[2] ARBIS D., & DIXIT V. V Game theoretic model for lane changing: Incorporating conflict risks. *Accident Analysis & Prevention*, 2019, 125: 158–164. https://doi.org/10.1016/j.aap.2019.02.007

[3] LI K., WANG X., XU Y., and WANG J. Lane changing intention recognition based on speech recognition models. *Transportation Research Part C: Emerging Technologies*, 2016, 69: 497–514. https://doi.org/10.1016/j.trc.2015.11.007

[4] XIE D. F., FANG Z. Z., JIA B., and HE Z. A data-driven lane-changing model based on deep learning. *Transportation Research Part C: Emerging Technologies*, 2019, 106: 41–60. https://doi.org/10.1016/j.trc.2019.07.002

[5] TREIBER M., & KESTING A. Microscopic calibration and validation of car-following models – a systematic approach. *Procedia - Social and Behavioral Sciences*, 2013, 80: 922–939. https://doi.org/10.1016/j.sbspro.2013.05.050

[6] YANG M., WANG X., and QUDDUS M. Examining lane change gap acceptance, duration and impact using naturalistic driving data. *Transportation Research Part C: Emerging Technologies*, 2019, 104: 317–331. https://doi.org/10.1016/j.trc.2019.05.024

[7] BALAL E., LONG R., and SARKODIE-GYAN T. A binary decision model for discretionary lane changing move based on fuzzy inference system. *Transportation Research Part C: Emerging Technologies*, 2016, 67: 47–61. https://doi.org/10.1016/j.trc.2016.02.009

[8] SHEN P., ZHANG X., and FANG Y. Essential Properties of Numerical Integration for Time-Optimal Path-Constrained Trajectory Planning. *IEEE Robotics and Automation Letters*, 2017, 2(2): 888–895. https://doi.org/10.1109/LRA.2017.2655580

[9] YANG D., ZHENG S., WEN C., JIN P. J., and RAN B. A dynamic lane-changing trajectory planning model for automated vehicles. *Transportation Research Part C: Emerging Technologies*, 2018, 95: 228–247. https://doi.org/10.1016/j.trc.2018.06.007

[10] ZHOU B., WANG Y., YU G., and WU X. A lane-change trajectory model from drivers' vision view. *Transportation Research Part C: Emerging Technologies*, 2017, 85: 609–627. https://doi.org/10.1016/j.trc.2017.10.013

[11] GONZÁLEZ D., PÉREZ J., MILANÉS V., and NASHASHIBI F. A Review of Motion Planning Techniques for Automated Vehicles. *IEEE Transactions on Intelligent Transportation Systems*, 2016, 17(4): 1135–1145. https://doi.org/10.1109/TITS.2015.2498841

[12] KAWABATA K., MA L., XUE J., and ZHENG N. A path generation method for automated vehicles based on Bezier curve. Proceedings of the IEEE/ASME International Conference on Advanced Intelligent Mechatronics, Wollongong, 2013, pp. 991–996. https://doi.org/10.1109/AIM.2013.6584223

[13] WU C., & CHIU Z. Simulations for Time-Optimal Trajectory Planning along Parametric Polynomial Lane-Change Curves for a Unicycle. Proceedings of the IEEE International Conference on Robotics and Biomimetics, Macau, 2017, pp. 2173–2178. https://doi.org/10.1109/ROBIO.2017.8324741

[14] RAHMAN M., ISMAIL M. T., AWANG N., and ALI M. K. M. A New Parametric Function-Based Dynamic Lane Changing Trajectory Planning and Simulation Model. *Pertanika Journal of Science and Technology*, 2021, 29(1): 217–232. http://dx.doi.org/10.47836/pjst.29.1.12

[15] LUO Y., XIANG Y., CAO K., and LI K. A dynamic automated lane change maneuver based on vehicle-to-vehicle communication. *Transportation Research Part C: Emerging Technologies*, 2016, 62: 87–102. https://doi.org/10.1016/j.trc.2015.11.011

[16] NTOUSAKIS I. A., NIKOLOS I. K., and PAPAGEORGIOU M. Optimal vehicle trajectory planning in the context of cooperative merging on highways. *Transportation Research Part C: Emerging Technologies*, 2016, 71(4): 464–488. https://doi.org/10.1016/j.trc.2016.08.007

[17] WANG C., & ZHENG C. Q. Lane change trajectory planning and simulation for intelligent vehicle. *Advanced Materials Research*, 2013, 671–674: 2843–2846. https://doi.org/10.4028/www.scientific.net/AMR.671-674.2843

[18] YOU F., ZHANG R., LIE G., WANG H., WEN H., and XU J. Trajectory planning and tracking control for autonomous lane change maneuver based on the cooperative vehicle infrastructure system. *Expert Systems with Applications*, 2015, 42(14): 5932–5946. https://doi.org/10.1016/j.eswa.2015.03.022

[19] WANG Y. Y., PAN D., LIU Z., and FENG R. *Study on Lane Change Trajectory Planning Considering of Driver Characteristics*, 2018. https://doi.org/10.4271/2018-01-1627
[20] WAGNER P., BUISSON C., and NIPPOLD R. Challenges in Applying Calibration Methods to Stochastic Traffic Models. *Transportation Research Record: Journal of the Transportation Research Board*, 2016, 2560(1): 10–16. https://doi.org/10.3141/2560-02
[21] ZHU M., WANG X., TARKO A., and FANG S. Modeling car-following behavior on urban expressways in Shanghai: A naturalistic driving study. *Transportation Research Part C: Emerging Technologies*, 2018, 93: 425–445. https://doi.org/10.1016/j.trc.2018.06.009
[22] VECHIONE M., BALAL E., and CHEU R. L. Comparisons of mandatory and discretionary lane changing behavior on freeways. *International Journal of Transportation Science and Technology*, 2018, 7(2): 124–136. https://doi.org/10.1016/j.ijtst.2018.02.002
[23] FEDERAL HIGHWAY ADMINISTRATION. Next Generation Simulation: Interstate US 101. *Freeway Dataset*, 2006. http://ngsim.fhwa.dot.gov/
[24] WAN Q., PENG G., LI Z., HIROSHI F., and INOMATA T. Spatiotemporal trajectory characteristic analysis for traffic state transition prediction near expressway merge bottleneck. *Transportation Research Part C: Emerging Technologies*, 2020, 117: 102682. https://doi.org/10.1016/j.trc.2020.102682
[25] LI L., CHEN X. M., and ZHANG L. A global optimization algorithm for trajectory data based car-following model calibration. *Transportation Research Part C: Emerging Technologies*, 2016, 68: 311–332. https://doi.org/10.1016/j.trc.2016.04.011
[26] PARK M., JANG K., LEE J., and YEO H. Logistic regression model for discretionary lane changing under congested traffic. *Transportmetrica A: Transport Science*, 2015, 11(4): 333–344. https://doi.org/10.1080/23249935.2014.994686
[27] ALI Y., ZHENG Z., HAQUE M., and WANG M. A game theory-based approach for modelling mandatory lane-changing behaviour in a connected environment. *Transportation Research Part C: Emerging Technologies*, 2019, 106: 220–242. https://doi.org/10.1016/j.trc.2019.07.011
[28] KANG K., & RAKHA H. A. Game theoretical approach to model decision making for merging maneuvers at freeway on-ramps. *Transportation Research Record: Journal of the Transportation Research Board*, 2017, 2623(1): 19–28. https://doi.org/10.3141/2623-03

参考文:

[1] MORIDPOUR S.、SARVI M.、ROSE G. 和 MAZLOUMI E. 重型车辆驾驶员换道决策模型。智能交通系统杂志：技术、规划和运营，2012年，16(1)：24–35。https://doi.org/10.1080/15472450.2012.639640
[2] ARBIS D., & DIXIT V.V 变道博弈论模型：纳入冲突风险。事故分析与预防，2019，125：158–164。https://doi.org/10.1016/j.aap.2019.02.007
[3] LI K., WANG X., XU Y., 和 WANG J. 基于语音识别模型的换道意图识别。交通研究C部分：新兴技术，2016年，69：497–514。https://doi.org/10.1016/j.trc.2015.11.007
[4] 谢东峰，方志忠，贾斌，何Z.一种基于深度学习的数据驱动换道模型。交通研究 C 部分：新兴技术，2019，106：41-60。https://doi.org/10.1016/j.trc.2019.07.002
[5] TREIBER M., & KESTING A. 跟车模型的微观校准和验证——一种系统方法。普罗塞迪亚-社会和行为科学，2013，80：922–939。https://doi.org/10.1016/j.sbspro.2013.05.050
[6] YANG M., WANG X., 和 QUDDUS M. 使用自然驾驶数据检查换道间隙接受度、持续时间和影响。交通研究C部分：新兴技术，2019年，104：317–331。https://doi.org/10.1016/j.trc.2019.05.024
[7] BALAL E.、LONG R.、SARKODIE-GYAN T. 基于模糊推理系统的自主变道运动二元决策模型。交通研究C部分：新兴技术，2016年，67：47–61。https://doi.org/10.1016/j.trc.2016.02.009
[8] 沉鹏，张旭，方勇。时间最优路径约束轨迹规划数值积分的基本性质。IEEE机器人与自动化快报，2017年，2(2)：888–895。https://doi.org/10.1109/LRA.2017.2655580
[9] 杨丹，郑松，文成，金鹏杰，冉斌。自动驾驶汽车动态换道轨迹规划模型。交通研究C部分：新兴技术，2018，95：228–247。https://doi.org/10.1016/j.trc.2018.06.007
[10] 周B.，王Y.，余刚，吴X. 驾驶员视野下的换道轨迹模型。交通研究C部分：新兴技术，2017年，85：609–627。https://doi.org/10.1016/j.trc.2017.10.013
[11] GONZÁLEZ D.、PÉREZ J.、MILANÉS V. 和 NASHASHIBI F. 自动车辆运动规划技术综述。IEEE智能交通系统汇刊，2016年，17(4)：1135–1145。https://doi.org/10.1109/TITS.2015.2498841
[12] KAWABATA K., MA L., XUE J., ZHENG N. 一种基于贝塞尔曲线的自动驾驶车辆路径生成方法。IEEE/美国机械工程师协会国际先进智能机电一体化会议论文集，卧龙岗，2013年，第991–996页。https://doi.org/10.1109/AIM.2013.6584223
[13] WU C., & CHIU Z. 独轮车沿参数多项式变道曲线的时间最优轨迹规划模拟。IEEE国际机器人与仿生学会议论文集，澳门，2017年，第2173-2178页。https://doi.org/10.1109/ROBIO.2017.8324741
[14] RAHMAN M.、ISMAIL M.T.、AWANG N. 和 ALI M.K.M. 一种新的基于参数函数的动态变道轨迹规划和仿真模型。佩塔尼卡科学技术杂志，2021，29(1)：217–232。http://dx.doi.org/10.47836/pjst.29.1.12
[15] 罗Y.，向Y.，曹K.，李K. 基于车车通信的动态自动变道策略。交通研究 C 部分：新兴技术，2016年，62：87–102。https://doi.org/10.1016/j.trc.2015.11.011
[16] NTOUSAKIS I.A.、NIKOLOS I.K. 和 PAPAGEORGIOU M. 高速公路合作并道背景下的最优车辆轨迹规划。交通研究C部分：新兴技术，2016，71(4)：464–488。https://doi.org/10.1016/j.trc.2016.08.007
[17] 王成，郑成群. 智能车辆换道轨迹规划与仿真. 先进材料研究，2013，671–674：2843–2846。https://doi.org/10.4028/www.scientific.net/AMR.671-674.2843
[18] 尤峰，张瑞，列刚，王辉，文辉，徐健。基于协同车辆基础设施系统的自主换道轨迹规划与跟踪控制。专

家系统与应用，2015，42(14)：5932–5946。https://doi.org/10.1016/j.eswa.2015.03.022

[19]王Y.Y.，潘丹，刘Z.，冯瑞.考虑驾驶员特征的换道轨迹规划研究，2018。https://doi.org/10.4271/2018-01-1627

[20] WAGNER P.、BUISSON C. 和 NIPPOLD R. 将校准方法应用于随机流量模型的挑战。交通研究记录：交通研究委员会杂志，2016年，2560(1)：10–16。https://doi.org/10.3141/2560-02

[21] 朱明，王X，塔科A，方S. 上海城市快速路跟车行为建模：自然主义驾驶研究。交通研究C部分：新兴技术，2018，93：425–445。https://doi.org/10.1016/j.trc.2018.06.009

[22] VECHIONE M.、BALAL E. 和 CHEU R. L. 高速公路上强制和自主变道行为的比较。国际交通科学与技术杂志，2018，7(2)：124–136。https://doi.org/10.1016/j.ijtst.2018.02.002

[23] 联邦公路管理局。下一代模拟：美国101号州际公路。高速公路数据集，2006年。http://ngsim.fhwa.dot.gov/

[24] WAN Q., PENG G., LI Z., HIROSHI F., 和 INOMATA T. 高速公路合流瓶颈附近交通状态转变预测的时空轨迹特征分析。交通研究C部分：新兴技术，2020年，117：102682。https://doi.org/10.1016/j.trc.2020.102682

[25] 李丽，陈晓明，张丽。一种基于轨迹数据的跟驰模型标定全局优化算法。交通研究C部分：新兴技术，2016年，68：311–332。https://doi.org/10.1016/j.trc.2016.04.011

[26] PARK M.、JANG K.、LEE J. 和 YEO H. 拥堵交通下自主换道的物流回归模型。运输计量A：交通科学，2015，11(4)：333–344。https://doi.org/10.1080/23249935.2014.994686

[27] ALI Y.，ZHENG Z.，HAQUE M.，和 WANG M. 基于博弈论的方法，用于对互联环境中的强制换道行为进行建模。交通研究C部分：新兴技术，2019年，106：220–242。https://doi.org/10.1016/j.trc.2019.07.011

[28] KANG K., & RAKHA H. A. 高速公路入口匝道合并操作模型决策的博弈论方法。交通研究记录：交通研究委员会杂志，2017年，2623(1)：19–28。https://doi.org/10.3141/2623-03